

CEBAF PROPOSAL COVER SHEET

This Proposal must be mailed to:

CEBAF
Scientific Director's Office
12000 Jefferson Avenue
Newport News, VA 23606

and received on or before 1 October 1991.

A. TITLE:

$\pi d \rightarrow pn$ Reaction Asymmetry Cross-Section Measurements

B. CONTACT
PERSON:

V.B. Ganeenko, Kharkov

(U.S. Contact Person: R. Gilman, Rutgers/CEBAF)

electronic mail: GILMAN@CEBAF

Phone: (804) 249-7011, (908) 932-5439

ADDRESS, PHONE, AND
ELECTRONIC MAIL
ADDRESS:

Institute Physics and Technology
Ukrainian Academy of Sciences
U-320108, Kharkov Phone: (057) 235-19-93
U.S.S.R. FAX: (057) 235-17-38

C. IS THIS PROPOSAL BASED ON A PREVIOUSLY SUBMITTED PROPOSAL OR LETTER OF INTENT?

☐

YES

☒

NO

IF YES, TITLE OF PREVIOUSLY SUBMITTED PROPOSAL OR LETTER OF INTENT

(CEBAF USE ONLY)

Receipt Date 1 Oct 91

Log Number Assigned PR-91-012

By L. S. Smith

RESEARCH PROPOSAL FOR CEBAF PAC5
 $\gamma d \rightarrow pn$ REACTION ASYMMETRY CROSS-SECTION MEASUREMENTS

K. A. Aniol¹, E. Cisbani⁵, C. C. Chang¹⁰, M. B. Epstein¹
J. M. Finn³, S. Frullani⁵, V. B. Ganenko⁶ (Spokesperson),
F. Garibaldi⁵, F. Ghio⁵, Shalev Gilad⁷,
R. Gilman^{2,8} (Spokesperson), C. Glashausser⁸, M. Jodice⁵,
L. Ya Kolesnikov⁶, G. Kumbartzki⁸, R. De Leo⁴,
G. J. Lolos¹¹, R. Lourie¹², P. Markovitz³, Z. Meziani⁹,
J. Mougey², R. Perrino⁴, R. Ransome⁸, A. L. Rubashkin⁶,
P. Rutt³, A. Saha², P. V. Sorokin⁶ (Spokesperson),
P. E. Ulmer², G. M. Urciuoli⁵, Yu V. Zhebrovskij⁶

¹The California State University at Los Angeles

²The Continuous Electron Beam Accelerator Facility

³The College of William and Mary in Virginia

⁴INFN Sezione Lecce

⁵INFN Sezione Sanita, Rome

⁶Kharkov Institute of Physics and Technology

⁷Massachusetts Institute of Technology

⁸Rutgers University

⁹Stanford University

¹⁰The University of Maryland

¹¹The University of Regina

¹²The University of Virginia, Charlottesville

RESEARCH PROPOSAL CEBAF

$\gamma d \rightarrow pn$ REACTION ASYMMETRY CROSS-SECTION MEASUREMENTS

**V.B. Ganenko (Spokesperson), Yu.V. Zhebrovskij, L.Ya. Kolesnikov,
A.L. Rubashkin, P.V. Sorokin (Spokesperson)**

KHARKOV INSTITUTE OF PHYSICS AND TECHNOLOGY

ABSTRACT.

We propose to measure the asymmetry of the $d(\gamma, p)n$ reaction in the photon energy range $E_\gamma = 0.6-2.0$ GeV. These measurements allow one to study the validity of existing nuclear-physics models in high energy region, the non-nucleonic degrees of freedom and multi-quark configurations in the deuteron and the deuteron wave function at small distances. Experimental results will give the possibility to check the existence of the asymptotic scaling phenomenon in the deuteron photodisintegration reaction at high energies.

The experiment will become a constituent of the complex studies of the $d(\gamma, p)n$ reaction that has been suggested at CEBAF [1].

INTRODUCTION

During more than 50 years special attention has been paid to deuteron photodisintegration reaction



because it is a simplest nuclear process, the studies of which allow one to examine the fundamental ideas of nuclear and elementary particles of physics at all stages of their development.

At present the energies exceeding 0.5 GeV are thought to be most interesting for studies. Reaction mechanisms here are complicated and change essentially on increasing energy. In the range $E_\gamma \leq 1$ GeV one may probably succeed to describe this process in the frame of nucleon-meson theory. However up to now there is not solved the problem of wave function behavior at small (≤ 0.5 Fermi) distances, well as questions about the deuteron non-nucleonic degrees of freedom. In the range $E_\gamma > 1.4$ GeV, as it follows from the recent measurements at SLAC [2], reaction mechanisms due to inner structure of the deuteron nucleons are possible.

One should expect that the qualitatively new information about the process (1) in the energy range given ($E_\gamma > 0.5$ GeV) may be obtained as a result of studying polarization observables that are often more sensitive to reaction mechanism details and to theoretical models than the cross-sections. Specifically, it seems to be important to study the asymmetry of cross-sections

$$\Sigma = (d\sigma_{\parallel} - d\sigma_{\perp}) / (d\sigma_{\parallel} + d\sigma_{\perp}), \quad (2)$$

where $d\sigma_{\parallel(\perp)} = d\sigma_{\parallel(\perp)} / d\Omega$ is the reaction cross-section when the polarization vector is directed parallel (perpendicular) to the reaction plane. This experiment is interesting and relatively simple, therefore it may start at the initial stage of mastering the

accelerator and the experimental techniques, because:

a) it doesn't require large electron currents and therefore, deuteron targets with large cooling power;

b) it doesn't require complicated detecting system for detection of reaction products;

c) only relative measurements are required, absolute measurements are not;

d) there are no problems connected with proton spin rotation in spectrometer magnetic field, as well as with the polarization analyzer.

MOTIVATION

CEBAF proposals [1] cover in sufficient measure the status of the theoretical description of deuteron photodisintegration reaction and the foundation of the necessity of its experimental studies. In support of all these arguments we note only the following:

1. Experimental studies of the energy range 0.6-2 GeV are far from complete yet. The bulk of experimental data base now at hand is concentrated in the range of comparatively moderate energies E_γ 0.7-0.8 GeV. There are no polarization data in the range $E_\gamma > 1$ GeV.

2. Reaction (1) has been intensively studied during last 10 years at Kharkov Institute of Physics and Technology (KhIPT). There have been measured the differential cross-sections $d\sigma/d\Omega$, with the non-polarized bremsstrahlung photon beam, the cross-sections $d\sigma_{\parallel}/d\Omega$ and $d\sigma_{\perp}/d\Omega$ with polarized photons in the range 0.04-0.1 GeV [3], the asymmetry of cross-sections Σ in the energy range 0.04-0.6 GeV [3,4], the proton polarization P in the range 0.4-1 GeV [5]. There also have been performed measurements of the observable T_1 (polarization asymmetry) in the double polarization experiment (polarized beam-proton polarization) in the energy range 0.4-0.6 GeV [6].

3. Theoretical studies in the 0.6-2 GeV range are scarce and,

general, no model describes all experimental data in the energy range discussed. Thus, calculations [7,8] may more or less satisfactorily describe only differential cross-sections for angles θ_p^{cm} near 90° . Experimental data on cross-sections at small ($\theta_p^{cm} \leq 30^\circ$) and large ($\theta_p^{cm} \geq 140^\circ$) angles, as well as the data on polarization observables and Σ are described unsatisfactorily, Fig.1. The analysis of the theoretical works, as well as of calculations [8-10], in which an improvement of the agreement between theory and experiment on the assumption about the dibaryon resonances is made, has shown that calculations of one or two observables (cross sections, nucleon polarization) and their satisfactory agreement with the existing data are not, generally speaking, a proof that mechanisms of the reaction are correctly understood and model parameter values are correct. It is so because to describe the reaction (1) it is necessary, in principle, to construct a large number of independent amplitudes (12) containing also a large number of parameters that are unknown now. New measurements of a new observable lead, as a rule, to the necessity of reconsidering the theoretical representations, especially of calculations at energies higher than 0.3 GeV.

In such a situation it is especially important, in our opinion, not to increase the accuracy of measuring one or another observable but rather to increase a number of new independent observables measured.

Similar experiments at energies $E_\gamma \leq 1$ GeV are being planned at SLAC, MEA accelerators and others. In this connection it seems principally important to add to the CEBAF investigation program studying the reaction (1) the measurements of cross-section asymmetries with linear polarized photons at energies up to 2-3 GeV where, according to data of paper [2] a phenomenon of asymptotic scaling [1] may be observed already at $E_\gamma \geq 1.4$ GeV.

The theoretical calculations of polarization observables for the energy range are not published, regrettably. The conventional approaches in the asymptotic limit lead, probably, to zero effects.

some polarization observables, for example P , T . As to cross section asymmetry, its value, if assumption about asymptotic scaling [11] is true, may be, in principle equal ~ 1 (or -1 , depending on relative sign phase of amplitude deuteron photodisintegration). The existing experimental data on proton polarization [5] and asymmetry [4], covering the energy range up to 1 GeV show that the proton polarization (0.7-0.8) is sufficiently large but the asymmetry is small (~ 0.2) and tends to diminish on increasing energy. However the data need checking. The calculations performed recently in Kharin [13] point to the specific sensitivity of the cross-section asymmetry to the Roper configuration in the deuteron wave function. Its accuracy influences very strongly the asymmetry value at $E_\gamma \approx 1-1.2$ GeV, decreasing it from 0.7 to 0.2.

On the whole, the experimental check of similar qualitative conclusions about the behavior of polarization observables in the above energy range is of special interest and may be effective test of the assumption about asymptotic scaling [11].

GENERAL DESCRIPTION OF THE EXPERIMENT

It is proposed to measure the cross-section asymmetry of $d(\gamma, p)n$ reaction in the photon energy range $E_\gamma = 0.6-2.0$ GeV for angles $\theta_p^{cm} = 30^\circ, 60^\circ, 90^\circ, 120^\circ, 150^\circ$.

The measurements in the vicinity of the lower boundary of the energy range are performed for comparison with existing data. Measurements in the region of 2 GeV may be possible to perform in the near future only at CEBAF.

The experiment is to be performed with the linearly polarized photons obtained from electron coherent bremsstrahlung in diamond single crystal. The separation of the reaction studied from the background of competing processes is accomplished by requiring coincidences.

EXPERIMENTAL TECHNIQUE AND PROCEDURE

The parameters of the CEBAF accelerator designed are advantage for the successful performing of the experiment: high duty fact high current and initial energy of electrons and small dimensions the beam spot.

The suggested scheme of the experiment is shown in Fig. 2. electron beam is brought into the diamond monocrystal fixed goniometric set. The deuterium target is located at the sm distance $\sim 0.8-1$ m from the photon target. Since the deuteron target this experimental scheme is irradiated with photons and electro measurements are necessary to subtract the contribution due electrodisintegration processes. Measurements may also be necess with the empty deuteron target to determine the contribution from target walls.

In the experiment it is suggested to use a liquid deuter target 10 cm long ($t_D = 0.0142X_0$) capable of the electron currents to 60 μ A.

Calculations of expected yields of pn coincidences from deuter photo- and electrodisintegration reactions have shown, that the photon target thickness should amount to not less than $\sim 0.05 - 0.06X_0$ achieve the desired $< 50\%$ value of the electrodisintegrati contribution to the full yield ratio. If one uses a diamond monocrystal as a photon target ($X_0 = 12.8$ cm), which is most frequent used to obtain the polarized photons because of the high De temperature, its thickness may be ~ 6 mm.

If the monocrystal target is oriented with respect to electron beam in such a way that the main contribution to the coherent bremsstrahlung cross-section was made by one point of the inverse lattice $(2, \bar{2}, 0)$ then the expected photon spectra and the radiation polarization for some energy values of the coherent bremsstrahlung peak are shown in Fig. 3 at the initial energy of electrons $E_0 = 4$ GeV. The $(2, \bar{2}, 0)$ orientation is most often used in experiments because

allows one to obtain higher polarization than other possible orientations.

CRYSTAL ORIENTATION AND POLARIZATION DETERMINATION

Crystal orientation is a procedure consisting of aligning the beam axis \vec{P}_0 with one of the main crystal axes, e.g. with $\vec{B}_1 = \langle 110 \rangle$ and with the other two axes $\vec{B}_2 = \langle 1\bar{1}0 \rangle$ and $\vec{B}_3 = \langle 001 \rangle$ directed along the horizontal and vertical rotation axes of the goniometer. On realizing it one usually performs special measurements of orientation dependencies of the photon beam intensity with an ionization chamber, or a quantometer, or pair spectrometer. Because experimental halls "A" are not equipped with magnets to clean the photon beam from the electron contamination, this conventional technique cannot be applied.

In such situation, in our opinion, for the hall "A" conditions the most promising is a some modification of the conventional method. For its realization in the hall "A" CEBAF, it is necessary to deflect the electron beam, after its passage through the single crystal, by a small bending magnet so, that the beam on its way to the beam dump should pass by the ionization chamber, fig.4. Bending magnet is installed directly after the deuteron target. Ionization chamber measuring 20×20 mm is placed at hall "A" exit (about 20-25 m from deuteron target). There is a deflection the electron beam on angle of ~ 5 mrad provide the displacement it on the distance of 100-120 mm at the region of the ionization chamber. The angle of the multiple scattering of the electron beam after its passage through the diamond single crystal and deuteron target consist of about 1 mrad for electron energy 4 GeV.

In order to deflect the electron beam with energy 4 GeV at angle about 5 mrad it is enough to have a magnet with field about 5 kilogauss and length of magnetic path ~ 13 cm. In such case electrons of the beam with energies $E_0 \geq 1.05$ GeV will get in beam dump of the

hall "A" ($E_0 \approx 1.05$ GeV correspond point A on fig 4), which according to design have long about 30 m and diameter ~ 2 m, and the electron with energy $E_0 \geq 0.5$ GeV will get in the tunnel of beam dump ($E_0 \approx 0.5$ GeV correspond point B). So practically all electron beam shall get in the tunnel of the beam dump. Besides, expediently the orientation of the crystals may carry out on lower intensity of the beam $\sim 0.01 \mu\text{ka}$. The bending magnet may be switch off, when crystal orientation is finished.

The orientation dependencies of the collimated photon beam obtained with this arrangement on Kcharkov Linac (the deflected electron beam passed at a distance of ~ 20 cm from ionization chamber), turned out to be practically the same as those for the traditional experimental set-up, fig.5.

It is suggested to determine the degree of photon polarization in the range of the coherent peak maximum from the measured orientation dependencies of reaction (1) yield $C_{\parallel(\perp)}(\theta_p, P_p, \theta, \alpha)$ at fixed values of kinematic variables θ_p and P_p (proton angle and momentum) corresponding to the photon energy value chosen, when the polarization vector is parallel (perpendicular) to the reaction plane. θ is the angle between the electron momentum \vec{P}_0 and \vec{B}_1 axis, α is the angle between the planes (\vec{P}_0, \vec{B}_1) and (\vec{B}_1, \vec{B}_2) . These angles are determined uniquely by the energy of the coherent peak in the bremsstrahlung spectrum. The effective polarization near the peak in the case when the main contribution to the bremsstrahlung cross-section is made by one point of the crystal inverse lattice $(2, \bar{2}, 0)$ equals, according to [4]:

$$P_\gamma = k \frac{2(1-X)}{[1 + (1-X)^2]} \cdot \frac{\beta - 1}{\beta}, \quad (3)$$

where $X = E_\gamma / E_0$, $\beta = (C_{\parallel}^{\max} + C_{\perp}^{\max}) / 2C_a$;

C_{\parallel}^{\max} - the proton yield in the maximum of the orientation dependence $C_{\parallel(\perp)}(\theta_p, P_p, \theta, \alpha)$,

C_a - the yield under the same kinematic conditions measured with non-oriented crystal.

The coefficient K accounts for the small contribution into coherent bremsstrahlung cross-section from the other points of diamond inverse lattice and it changes from 0.98 to 0.9 on changing from 0.1 to 0.4. |

THE $\gamma d \rightarrow pn$ REACTION IDENTIFICATION

In contrast to SLAC experiment [2] where measurements have been performed at the end of the photon bremsstrahlung spectrum, in experiment suggested it is necessary to measure the reaction yields due to photons from the coherent peak which must be at relative energy $X \leq 0.5$ to have the sufficiently high photon polarization.

Therefore the conditions for the reaction identification will differ essentially. To separate reaction (1) from the background it is necessary to use the pn coincidence technique in this case. To detect protons it is suggested to use the detector assembly for H spectrometer in hall "A".

For neutron registering one can use a hodoscope consisting of counters out of plastic scintillator 20 cm thick, 10 cm wide and 16 cm high (the overall size of the hodoscope is 30 cm horizontally 65 cm vertically) placed 5 m from the deuteron target center. Geometric dimensions given allow one to couple the solid angles of proton and neutron arms when registering pn coincidences at angle 90° . In front of every neutron counter of the hodoscope there are coincidence scintillation counters with dimensions $10 \times 16.25 \times 1$ cm³ placed to suppress the charged particle background.

The neutron telescope is located on the rotating platform inside a shield of concrete blocks. In front of it a lead absorber 10 cm thick ($17.68X_0$) is placed to lower the counter load with charged particles and photons. For a more reliable separation of the deuteron photodisintegration channel one can measure neutron energies using time-of-flight technique, together with the angles. Time resolution

of 0.3 nsec will give energy resolution not worse than 10% in energy range studied.

ESTIMATES OF PROTON AND NEUTRON COUNTING RATES

Counting rates of proton and neutron channels have been estimated for the angles $\theta_p^{cm} = 30^\circ, 60^\circ, 90^\circ, 120^\circ, 150^\circ$ in the photon energy range 0.6-2 GeV. The corresponding kinematic conditions are listed in Table 1.

In calculations one has assumed that:

- the solid angle of the HRHS spectrometer for proton is 7×10^{-3} sr, the momentum acceptance $\Delta p/p = 0.05$;
- deuteron target is 10 cm thick (0.51×10^{24} nuclei per cm^2);
- inlet and outlet windows are 0.1 mm aluminum thick (1.20×10^{24} nuclei per cm^2);
- neutron detection efficiency is 0.2;
- neutron transmission coefficient in the 10 cm lead filter is 0.57;
- detection efficiency in proton arm is 100%;
- diamond monocrystal is 6 mm thick. Energy of the primary electron beam is 4 GeV.

To calculate the $d(\gamma, p)n$ reaction yield one has evaluated number of real photons for an oriented and disoriented diamond crystal in the photon energy range determined by the reaction kinematics and particle acceptance over momenta $\Delta p/p = 0.05$.

Data on the differential cross section of the $d(\gamma, p)n$ reaction for $\theta_p^{cm} = 90^\circ$ have been taken from the CEBAF proposal [11] and ones at the 2 GeV energy have been obtained by their extrapolation. Table 1 lists the cross section values. Data on the differential cross sections at angles $30^\circ, 60^\circ, 120^\circ$ and 150° have been taken the same as for 90° .

For angle 30° the calculation also have been done

differential cross section, which may be obtained from the theoretical approach [13]. In this approach the cross section at $\theta_p^{cm} = 30^\circ$ proved to be about 2.3 times for $E_\gamma = 1$ GeV and about 7.5 times for $E_\gamma =$ GeV greater than cross sections at $\theta_p^{cm} = 90^\circ$. For other photon energies cross sections have been obtained by interpolation. The results are listed in Tables (under name variant 2).

To calculate double differential cross sections of concurrent reactions for photons and electrons interacting with deuterium and aluminum (only for $\theta_p^{cm} = 90^\circ$) nuclei, we have used codes of Lightbown and O'Connell [14]. There is no calculation of proton and pion yields from target's wall for other angles, because it is small (5-10%). The number of equivalent photons has been calculated for the disoriented diamond target 6 mm thick.

Table II gives the results of calculating the proton channel counting rates resulting from the interaction of bremsstrahlung ($d(\gamma, p)n$, amorp.) and coherent photon beams ($d(\gamma, p)n$, crystal) with the deuterium target, as well as proton and pion yields from photon and electron beams together with the total counting rates (total π , total p). Proton counting rates with the mixed $e+\gamma$ beam incident on the oriented (total p, crystal) and disoriented (total p, amorp. crystal) target are mainly due to the deuterium target, with the contribution from the electron component of the beam predominant. One sees from the last three columns that the proton channel counting rates do not exceed $3 \times 10^3 \text{ sec}^{-1}$ for angles $\theta_p^{cm} \geq 60^\circ$. Under these conditions the detector system will provide rejection of pions as well as positrons and other particles. For $\theta_p^{cm} = 30^\circ$ the expected counting rate is considerably larger. Probably big counting rates do not allow to use electron currents more than about 5 μA . The expected counting rate for proton (total p, crystal) is about $\sim 10^4 \text{ sec}^{-1}$ for $\theta_p^{cm} = 30^\circ$ and for other angles does not exceed 3000 sec^{-1} .

The neutron counter counting rate caused by as many neutrons as charged particles. It has been estimated by integrating proton, pion and neutron spectra calculated according to the code [15] over the

momentum range 50-1700 MeV/c accounting for particle absorption in the lead absorber and for neutron detecting efficiency. The energy of the primary electron beam is 4 GeV.

The counting rates of each of 12 counters of the neutron hodoscope by charged (π, p) particles and neutrons from photons and electrons are given in Table III. The contribution from the target walls is insignificant and has not been accounted for. The total counting rates (total p, π, n) of the neutron block is, mainly, due to π -mesons. The neutron counting rate (total, n) is of order of magnitude less. Thus, the counting rates of every neutron counter will not exceed $\sim 10^6 \text{ sec}^{-1}$. For the conventional electronics speed $\leq 10^{-8} \text{ s}$ in a separate block one will provide effective rejection of charged particles.

Estimates based on the experimental data at Bates was the neutron flux $2.2 \times 10^3 \text{ n/s } \mu\text{KA msr gr cm}^{-2}$ at the angle 56.6° for the electron energies 762 MeV from the deuterium target, and with the account of absorption in lead and counter efficiency give counting rates $\approx 2 \times 10^2$ which agrees with $d(e, n)\gamma$ estimates of Table III to the order of magnitude.

COUNTING RATE OF PROTON-NEUTRON COINCIDENCES

The counting rate of np coincidences has been calculated for the deuteron target under the assumption of full matching of solid angles of proton and neutron areas. One has accounted for neutron absorption by the lead absorber shield and the efficiency. There have been calculated yields at real photons from the disoriented ($d(\gamma, p)$ amorph) and oriented ($d(\gamma, p)n$, crystal) crystal as well as at virtual photons ($d(e, p)n$). Table IV gives the calculation results.

It is seen that for the oriented crystal the ratio of the $d(\gamma, p)n$ reaction yields to the $d(e, p)n$ yield on the e^- beam is considerably bigger than the corresponding ratio for the disoriented

crystal. The number of accidental coincidences has been estimated accounting for proton (total p, crystal) and neutron (total n) load of one block under the assumption that the resolution time for coincidences is $\sim 2 \times 10^{-9}$ sec. The ratio of accidental and true coincidences for all 12 blocks approaches 40% at high energies for angles $\theta_p^{cm} \geq 60^\circ$, Table V. At angle $\theta_p^{cm} = 30^\circ$ (for variant 1) the ratio may be some greater.

STATISTICS AND BEAM TIME

If one neglects the contribution from background coincidences from the empty target, then in our scheme of experiment one needs to measure the number of pn coincidences:

- with the mixed $\gamma + e$ beam when the polarization vector is parallel C_{\parallel} and perpendicular C_{\perp} to the reaction plane as well as for the disoriented crystal C_a ;

- with the electron beam C_e (without the photon target).

The asymmetry value will be determined by the expression:

$$\Sigma = \frac{1}{P_{\gamma}} \frac{C_{\parallel} - C_{\perp}}{C_{\parallel} + C_{\perp} - 2C_e} \quad (4)$$

and the polarization P_{γ} value according to (3) from data on $C_{\parallel} - C_e$, $C_{\perp} - C_e$ and $C_a - C_e$. The necessary statistics for values of $C_{\parallel} + C_{\perp}$, C_a and C_e providing the measurement accuracy $\Delta \Sigma_{\gamma} = \pm 0.05$ and pure beam time are listed in Table V. Starting from these values and corresponding counting rates of coincidences given in Table IV (total np, crystal), (total np)' and d(e, p)n the pure beam time is estimated for every energy and angle. Data are given in Table V.

In estimates we have used the calculated photon polarization values P_{γ} . Σ values at energies < 1 GeV and $\theta_p^{cm} = 90^\circ$ have been taken

from [12] and at larger energies they have been fixed arbitrarily value $\Sigma = 0.15$. Σ -values for other angles have been fixed at the same value too. It should be said, that C values depend weakly on Σ values.

At angle 30° measurements would be reasonable to limit by range 0.6-1.6 GeV, if cross sections in this angle the same as at 9° (variant 1). If the theoretical calculation [13] is true, then measurements may be carried out up to 2 GeV (variant 2). The pure beam time of measurements at all five angles would amount ≈ 87 hours (variant 1) ≈ 76 hours (variant 2). The estimates given will be corrected in the process of detailed simulation of the experiment and of accumulation of the experience of working with all the apparatus complex.

It is necessary to have additional beam time for:

- tests, apparatus calibration ~ 50 hours;
- changing the coherent peak energy, the angle, the magnet field ~ 80 hours;
- measurements with the empty target, ~ 50 hours;
- control of results reproduction, ~ 40 hours.

Thus the total beam time for the experiment proposed is estimated 300 hours.

EXPERIMENTAL VERIFICATION

Experimental verification of the measurement Σ -asymmetry on mixed $\gamma + e^-$ beam in one arm was carried out in Kharkov Linac. The experimental layout was the same as is shown on fig.4. We used diamond single crystal with 1.8 mm thickness, which was orientated in the experimental hall on mixed $\gamma + e^-$ beam using the method supposed for hall "A" fig 6 and performed in Kharkov. It was described above.

The conditions of the experiment:

- electron beam energy 1.7 GeV;
- angle of proton detection $\theta_p^{cm} = 90^\circ$;
- energy of coherent photon peak 300 MeV;

- target with two appendix by 40 mm in diameter and 200 mm 1
One of them was filled liquid deuterium, other liquid hydrogen.

The protons from the reaction (1) were detected by magn spectrometer and telescope of scintillation counters.

The spectra of intensity the γ -radiation and its polarization our experimental conditions were calculated and shown on fig.6.

Orientation dependencies of proton yields from deut photodisintegration after electrodisintegration background subtrac are shown on fig 7 for two cases: when vector polarization the ph beam is parallel and perpendicular to reaction plane. The backgr of the deuteron electrodisintegration was $\approx 80-85\%$, that practic agree with calculation. The effective polarization calculated expression (3) was about 63%. Here can see that yield of the reac depend from direction of polarization vector of the beam. The valu the asymmetry obtained from our measurements agree with experime data [4], fig.1b.

RADIATION DAMAGE OF THE CRYSTAL

The working experience at the KHIPT Linac has shown the a irradiating diamond monocrystal with the $\sim 10^{20}$ electron/cm² dose crystal qualities may deteriorate up to its destruction. We may to perform all measurements with one or two monocrystals. Cry orientation, testing measurements, apparatus tuning should be done the lower electron intensities.

COLLABORATION CONDITIONS

The experiment proposed should be considered as a part of experime program on studying the $\gamma d \rightarrow pn$ process proposed to be performed in "A" [1]. And it may be performed simultaneously, e.g. with

experiment on proton polarization measurements using a part of the CEBAF experimental apparatus, i.e. spectrometer proton counting system, deuteron target, neutron detector.

The KHIPT will provide the device to obtain polarized photon. It also performs the preliminary orientation of diamond crystals at the Linac. This technique of asymmetry measurements with the mixed beam of electrons and photons at Kharkov will test in the energy range up to 0.8 GeV at angles $\theta_p^{cm} \geq 90^\circ$.

CONCLUSIONS

In conclusion one should note the following. First, the apparatus made for this proposal, allows one to measure the polarization parameters in reactions of photodisintegration of lightest nuclei: for example, cross-section asymmetries of reactions, as well as the polarization observable in double polarization experiments (polarized beam-proton polarization) for d, ^3He and ^4He nuclei.

Second, the location of the photon target at such a small distance (0.8-1 m) from the deuteron target is due, mainly, to the requirement not to disturb the hall "A" setting according to the project. It will be more advantageous, from the viewpoint of this experiment, to increase this distance up to 10-15 m and to install a sweeping magnet with beam dump. The beam size will increase by 3-4 mm, which is not critical, and one may perform the experiment without photon beam collimation i.e. without intensity losses. Such an experimental scheme would allow to get rid of measurements with the removed photon target, would decrease the beam time by a factor not less than 2, and would increase the accuracy of measurements. It would reduce also the requirements to the cooling power of the deuteron target and the background.

REFERENCES

1. Proposal CUBA: PR-89-012, PR-89-019, PR-89-020.
2. J. Napolitano et al. Phys. Rev. Lett., 61, 2530, 1988.
3. V.B. Ganenko et al. ZhETF Pis'ma, 50, 220, 1989 (In Russian).
4. V.G. Gorbenko et al. Yadernaya fizika (Nuclear Physics), 3
1073, 1982 (In Russian).
5. A.S. Bratashevsky et al. ibid., 32, 418, 1980 (In Russian);
ibid., 44, 960, 1986. (In Russian).
Nucl. Phys. A 451, 751, 1986.
6. V.P. Barannik et al. Yadernaya fizika 43, 785, 1986 (In Russian)
7. J.M. Laget, Nucl. Phys. A 312, 265, 1978.
8. H. Ikeda et al. Phys. Rev. Lett. 42, 1321, 1979.
9. Y. Ohashi et al. Phys. Rev. C 36, 2422, 1987.
10. V.P. Barannik, Yu.V. Kulish, Yadernaya fizika, 47, 1580, 1988
(In Russian).
11. S.J. Brodsky, G. Farrar, Phys. Rev. D 11, 1309, 1975.
12. F.V. Adamyant et al. Materials of the workshop on electromagnetic
interactions of hadrons and nuclear at intermediate energy
Nor-Amberd, October, 1990.
13. S.I. Nagorny, ibid.
14. J.W. Lightbody et al. Computers in Physics, May/June, 1988, p.57
15. K. Ogawa et al. Nucl. Phys. A 340, 451, 1980.

Table 1. Kinematic conditions of measurements.

$\theta_p^{cm} = 30^\circ$				$\theta_p^{cm} = 60^\circ$			
E_γ	θ_p^{Lab}	P_p	T_p	E_γ	θ_p^{Lab}	P_p	T_p
GeV	deg	GeV/c	GeV	GeV	deg	GeV/c	GeV
0.6	21.1	1.038	0.461	0.6	43.4	0.944	0.392
0.8	20.1	1.261	0.634	0.8	41.3	1.135	0.534
1.0	19.1	1.475	0.810	1.0	39.5	1.317	0.678
1.2	18.4	1.682	0.988	1.2	38.0	1.491	0.824
1.4	17.7	1.885	1.168	1.4	36.6	1.661	0.970
1.6	17.1	2.086	1.349	1.6	35.4	1.828	1.116
1.8	16.5	2.284	1.531	1.8	34.4	1.992	1.264
2.0	16.0	2.480	1.713	2.0	33.4	2.154	1.411

$\theta_p^{cm} = 90^\circ$				
E_γ	θ_p^{Lab}	P_p	T_p	$(d\sigma/d\Omega)_D^{Lab}$
GeV		GeV/c	GeV	nb/sr
0.6	68.2	0.806	0.299	247
0.8	65.2	0.953	0.399	98
1.0	62.7	1.089	0.499	41
1.2	60.5	1.218	0.599	18
1.4	58.6	1.342	0.699	8.3
1.6	56.8	1.462	0.799	4.1
1.8	55.3	1.580	0.899	2.4
2.0	53.9	1.695	0.999	1.0

Table 1 (continue).

$$\theta_p^{cm} = 120^\circ$$

$$\theta_p^{cm} = 150^\circ$$

E_γ GeV	θ_p^{Lab} deg	P_p GeV/c	T_p GeV
0.6	97.6	0.654	0.206
0.8	94.1	0.751	0.264
1.0	91.1	0.838	0.320
1.2	88.5	0.918	0.374
1.4	86.2	0.994	0.428
1.6	84.1	1.066	0.482
1.8	82.1	1.135	0.534
2.0	80.4	1.202	0.587

E_γ GeV	θ_p^{Lab} deg	P_p GeV/c	T_p GeV
0.6	134.5	0.525	0.18
0.8	131.7	0.579	0.18
1.0	129.1	0.624	0.18
1.2	126.8	0.662	0.20
1.4	124.7	0.697	0.20
1.6	122.8	0.728	0.20
1.8	121.0	0.757	0.20
2.0	119.3	0.785	0.20

Table II. Counting rates in the proton arm.

(targets wall)

E_γ GeV	I_e μka	$\text{Al}(\gamma, p)\text{X}$ sec^{-1}	$\text{Al}(e, p)\text{X}$ sec^{-1}	$\text{Al}(\gamma, \pi)\text{X}$ sec^{-1}	$\text{Al}(e, \pi)\text{X}$ sec^{-1}
$\theta_p^{\text{cm}} = 90^\circ$					
0.6	1	1.60	7.6	1.26	3.38
0.8	1	0.49	3.4	0.33	0.92
1.0	5	1.03	9.1	0.38	1.04
1.2	10	0.88	9.9	0.07	0.18
1.4	30	1.22	16.5	-	-
1.6	30	0.62	9.4	-	-
1.8	50	0.58	9.2	-	-
2.0	50	0.40	5.7	-	-

(deuteron)

E_γ GeV	I_e μA	$d(\gamma, p)n$ amorp sec^{-1}	$d(\gamma, p)n$ crystal sec^{-1}	$d(\gamma, p)\text{X}$ amorp sec^{-1}	$d(e, p)\text{X}$ sec^{-1}	$d(\gamma, \pi)\text{X}$ amorp sec^{-1}	$d(e, \pi)\text{X}$ sec^{-1}	total $\pi+p$ amorp sec^{-1}	total p amorp sec^{-1}
$\theta_p^{\text{cm}} = 90^\circ$									
0.6	1	25.6	79.9	-	129.6	80.1	207.0	456	164
0.8	1	9.7	28.6	-	70.2	21.2	56.7	163	84
1.0	5	19.4	53.1	-	195.8	24.3	63.0	314	225
1.2	10	16.3	40.8	-	305.6	4.8	11.7	349	333
1.4	30	21.5	46.7	-	430.6	-	-	470	470
1.6	30	10.6	22.3	-	128.2	-	-	149	149
1.8	50	10.3	20.2	-	108.0	-	-	128	128
2.0	50	4.2	8.1	-	65.5	-	-	76	76

Table II (continue).

E_γ	I_e	$d(\gamma, p)n$ amorp	$d(\gamma, p)n$ crystal	$d(\gamma, p)X$ amorp	$d(e, p)X$	$d(\gamma, \pi)X$ amorp	$d(e, \pi)X$	total $\pi+p$ amorp	total p amorp	total $\pi+p$ cry
GeV	μA	sec^{-1}	sec^{-1}	sec^{-1}	sec^{-1}	sec^{-1}	sec^{-1}	sec^{-1}	sec^{-1}	sec^{-1}

$$\theta_p^{\text{cm}} = 30^\circ \text{ (variant 1)}$$

0.6	1	19.5	61.2	5778	3987	11520	7731	29016	9765	126
0.8	1	7.20	21.2	4590	3033	8114	5139	20876	7623	98
1.0	1	2.80	7.64	3538	2236	5867	3512	15153	5774	74
1.2	2	2.29	5.72	5224	3220	8161	4685	21290	8444	104
1.4	4	1.97	4.28	7645	4640	11470	6300	30055	12275	144
1.6	2	0.48	1.01	2759	1681	3942	2099	10481	4440	47
1.8	1	0.14	0.27	995	623	1367	698	3683	1618	17
2.0	1	0.05	0.11	703	471	903	448	2525	1174	12

$$\theta_p^{\text{cm}} = 30^\circ \text{ (variant 2)}$$

0.6	1	19.5	61.2	5778	3987	11520	7731	29016	9765	126
0.8	1	7.20	21.2	4590	3033	8114	5139	20876	7623	98
1.0	1	6.51	17.8	3538	2236	5867	3512	15153	5774	74
1.2	2	7.56	18.9	5224	1610	8161	4685	21290	8444	104
1.4	4	8.57	18.6	7645	4640	11470	6300	30055	12275	144
1.6	5	6.44	13.6	6898	4203	9855	5247	26203	11101	111
1.8	5	4.32	8.64	4977	3114	6926	3488	18505	8091	81
2.0	4	1.62	3.24	2812	1883	3611	1793	10099	4695	48

Table II (continue).

E_γ	I_e	$d(\gamma, p)n$ amorp	$d(\gamma, p)n$ crystal	$d(\gamma, p)X$ amorp	$d(e, p)X$	$d(\gamma, \pi)X$ amorp	$d(e, \pi)X$	total $\pi+p$ amorp	total p amorp	total p crys
GeV	μA	sec^{-1}	sec^{-1}	sec^{-1}	sec^{-1}	sec^{-1}	sec^{-1}	sec^{-1}	sec^{-1}	sec^{-1}

$$\theta_p^{\text{cm}} = 60^\circ$$

0.6	1	21.6	67.5	1130	1209	950	1110	4399	2339	288
0.8	1	8.04	23.8	674	695	368	414	2151	1369	169
1.0	3	9.45	25.9	1160	1193	540	586	3479	2353	291
1.2	5	6.52	16.3	1066	1166	439	461	3132	2232	263
1.4	10	5.65	12.3	1170	1431	441	517	3559	2601	289
1.6	10	2.76	5.80	610	803	210	202	1825	1413	147
1.8	30	4.75	9.36	869	999	268	245	2381	1868	194
2.0	30	1.94	3.62	399	486	98	81	1064	885	91

$$\theta_p^{\text{cm}} = 120^\circ$$

0.6	1	32.3	101.0	-	112	4.3	174	322.6	144.3	213
0.8	1	12.8	37.6	-	64	-	-	76.8	76.8	101
1.0	2	10.5	28.6	-	93	-	-	103.5	103.5	121
1.2	5	11.3	28.2	-	189	-	-	200.3	200.3	217
1.4	20	20.2	44.1	-	428	-	-	448.2	448.2	472
1.6	30	15.0	32.0	-	381	-	-	396.0	396.0	413
1.8	30	9.00	17.7	-	294	-	-	303.0	303.0	311
2.0	50	6.26	11.7	-	311	-	-	317.3	317.3	322

Table II (continue).

E_γ	I_e	$d(\gamma, p)n$ amorp	$d(\gamma, p)n$ crystal	$d(\gamma, p)X$ amorp	$d(e, p)X$	$d(\gamma, n)X$ amorp	$d(e, n)X$	total $\pi+p$ amorp	total p amorp	total p crys
GeV	μkA	sec^{-1}	sec^{-1}	sec^{-1}	sec^{-1}	sec^{-1}	sec^{-1}	sec^{-1}	sec^{-1}	sec^{-1}
$\theta_p^{cm} = 150^\circ$										
0.6	1	42.3	132.2	-	92	-	-	-	134.3	224
0.8	1	17.6	51.9	-	56	-	-	-	73.6	107
1.0	2	15.2	41.5	-	85	-	-	-	100.2	126
1.2	5	17.0	42.5	-	170	-	-	-	187.0	212
1.4	10	15.8	34.5	-	285	-	-	-	300.8	319
1.6	20	16.5	34.5	-	494	-	-	-	510.5	528
1.8	30	14.9	29.5	-	661	-	-	-	675.9	690
2.0	30	6.40	12.0	-	606	-	-	-	612.4	618

Table III. Counting rates for one counter in the neutron arm.

θ_p^{cm}	θ_p^{Lab}	I_e	$d(\gamma, p)X$	$d(e, p)X$	$d(\gamma, n)X$	$d(e, n)X$	$d(\gamma, n)X$	$d(e, n)X$	total p, π, n	total n
deg	deg	μkA	sec^{-1}	sec^{-1}	sec^{-1}	sec^{-1}	sec^{-1}	sec^{-1}	sec^{-1}	sec^{-1}
30	133.5	1	-	2.81	797	138	54	261	1253	31
60	98.2	1	0.22	8.78	750	1462	88	294	2603	38
90	68.2	1	12.6	87	1917	3540	159	333	6049	49
90	53.9	1	235	512	4514	5008	283	482	11034	76
120	44.9	1	814	916	8972	10480	374	572	22128	94
150	21.2	1	5948	4109	37956	46062	1320	1170	96565	249

Table IV. Counting rates for pn coincidences.

E_γ	I_e	$d(\gamma,p)n$ amorp	$d(\gamma,p)n$ crystal	$d(e,p)n$	total pn amorp trues	total pn crystal trues	ratio amorp	ratio crystal	accl 10 ⁻
GeV	μA	sec ⁻¹	sec ⁻¹	sec ⁻¹	sec ⁻¹	sec ⁻¹	$\frac{d(\gamma,p)n}{d(e,p)n}$	$\frac{d(\gamma,p)n}{d(e,p)n}$	sec

$$\theta_p^{cm} = 30^\circ \text{ (variant 1).}$$

0.6	1	2.24	7.00	5.01	7.25	12.01	0.45	1.40	1.59
0.8	1	0.83	2.43	1.84	2.67	4.27	0.45	1.32	1.23
1.0	1	0.32	0.87	0.74	1.06	1.61	0.44	1.18	0.94
1.2	2	0.26	0.66	0.59	0.85	1.25	0.44	1.12	2.62
1.4	4	0.22	0.49	0.52	0.74	1.01	0.43	0.94	7.26
1.6	2	0.055	0.115	0.128	0.183	0.24	0.43	0.90	1.19
1.8	1	0.015	0.031	0.035	0.050	0.071	0.43	0.89	0.21
2.0	1	0.006	0.012	0.014	0.020	0.026	0.43	0.86	0.15

$$\theta_p^{cm} = 30^\circ \text{ (variant 2).}$$

0.6	1	2.24	7.00	5.01	7.25	12.01	0.45	1.40	1.59
0.8	1	0.83	2.43	1.84	2.67	4.27	0.45	1.32	1.23
1.0	1	0.75	2.02	1.71	2.46	3.73	0.44	1.18	0.94
1.2	2	0.86	2.21	1.97	2.83	4.18	0.44	1.12	2.62
1.4	4	0.98	2.13	2.27	3.21	4.40	0.43	0.94	7.26
1.6	5	0.74	1.55	1.72	2.46	3.27	0.43	0.90	7.43
1.8	5	0.49	1.02	1.15	1.65	2.17	0.43	0.89	5.26
2.0	4	0.19	0.37	0.43	0.62	0.80	0.43	0.86	2.44

Table IV (continue).

E_γ	I_e	$d(\gamma,p)n$ amorp	$d(\gamma,p)n$ crystal	$d(e,p)n$ sec ⁻¹	total pn amorp trues	total pn crystal trues	ratio amorp	ratio crystal	accid 10 ⁻²
GeV	μA	sec ⁻¹	sec ⁻¹	sec ⁻¹	sec ⁻¹	sec ⁻¹	$\frac{d(\gamma,p)n}{d(e,p)n}$	$\frac{d(\gamma,p)n}{d(e,p)n}$	sec ⁻¹

$$\theta_p^{cm} = 60^\circ$$

0.6	1	2.48	7.72	6.10	8.58	13.82	0.41	1.27	0.441
0.8	1	0.92	2.71	2.31	3.23	5.02	0.40	1.17	0.259
1.0	3	1.09	2.96	2.75	3.84	5.71	0.40	1.08	1.336
1.2	5	0.75	1.86	1.91	2.66	3.77	0.39	0.97	2.017
1.4	10	0.65	1.41	1.67	2.32	3.08	0.39	0.84	4.429
1.6	10	0.32	0.67	0.83	1.15	1.50	0.39	0.73	2.255
1.8	30	0.54	1.07	1.43	1.97	2.50	0.38	0.75	8.920
2.0	30	0.22	0.41	0.68	0.90	1.09	0.32	0.60	3.694

$$\theta_p^{cm} = 90^\circ$$

0.6	1	2.93	9.14	7.08	10.01	16.22	0.41	1.29	0.042
0.8	1	1.12	3.28	2.90	4.02	6.18	0.39	1.13	0.021
1.0	5	2.22	6.08	6.23	8.45	12.31	0.36	0.98	0.292
1.2	10	1.86	4.66	5.51	7.37	10.17	0.34	0.85	0.857
1.4	30	2.46	5.34	7.72	10.18	13.06	0.32	0.69	3.836
1.6	30	1.22	2.55	4.12	5.34	6.67	0.30	0.62	1.300
1.8	50	1.17	2.32	4.07	5.24	6.39	0.29	0.57	1.967
2.0	50	0.49	0.93	1.72	2.21	2.65	0.28	0.54	1.283

Table IV (continue).

E_γ	I_e	$d(\gamma,p)n$ amorp	$d(\gamma,p)n$ crystal	$d(e,p)n$	total pn amorp trues	total pn crystal trues	ratio amorp	ratio crystal	accid 10^{-2}
GeV	μKA	sec^{-1}	sec^{-1}	sec^{-1}	sec^{-1}	sec^{-1}	$\frac{d(\gamma,p)n}{d(e,p)n}$	$\frac{d(\gamma,p)n}{d(e,p)n}$	sec^{-1}

$$\theta_p^{\text{cm}} = 120^\circ$$

0.6	1	3.70	11.55	11.83	15.53	23.38	0.31	0.98	0.081
0.8	1	1.46	4.30	4.86	6.32	9.16	0.30	0.88	0.038
1.0	2	1.20	3.28	4.22	5.42	7.50	0.28	0.78	0.092
1.2	5	1.30	3.22	5.00	6.30	8.22	0.26	0.64	0.410
1.4	20	2.31	5.05	10.39	12.70	15.44	0.22	0.49	3.572
1.6	30	1.75	3.67	7.70	9.45	11.37	0.23	0.48	4.680
1.8	30	1.03	2.03	5.05	6.08	7.08	0.20	0.40	3.538
2.0	50	0.72	1.31	3.40	4.12	4.71	0.21	0.40	6.107

$$\theta_p^{\text{cm}} = 150^\circ$$

0.6	1	4.84	14.68	19.64	24.48	34.32	0.25	0.75	0.223
0.8	1	2.02	5.94	8.68	10.70	14.62	0.23	0.68	0.107
1.0	2	1.74	4.74	8.12	9.86	12.86	0.21	0.58	0.262
1.2	5	1.94	4.86	9.73	11.67	14.59	0.20	0.50	1.059
1.4	10	1.81	3.95	12.58	14.39	16.53	0.15	0.31	3.185
1.6	20	1.88	3.96	10.69	12.57	14.65	0.18	0.37	10.53
1.8	30	1.71	3.38	10.26	11.97	13.64	0.17	0.33	20.62
2.0	30	0.73	1.37	4.59	5.32	5.96	0.16	0.30	18.46

Table V. Statistic and beam time.

E_γ	I_e	P_γ	Σ	$C_{ } + C_{\perp}$	C_a	C_e	$\frac{\text{accid}}{\text{trues}}$	T
GeV	μA			counts	counts	counts	%	hours

$\theta_p^{\text{cm}} = 30^\circ$ (variant 1)

0.6	1	0.59	0.15	4510	642	941	1.59	0.18
0.8	1	0.56	0.15	5270	640	1138	3.45	0.58
1.0	1	0.53	0.15	6444	662	1473	7.01	1.84
1.2	2	0.50	0.15	7800	658	1861	25.2	2.82
1.4	4	0.47	0.15	10236	662	2632	86.3	4.47
1.6	2	0.45	0.15	11586	664	3026	59.5	21.0
1.8	1	0.40	0.15	15686	673	4228	37.6	98.7
2.0	1	0.35	0.15	21823	679	6029	67.6	362.2
total								491.79
0.6-1.6 GeV total								30.89

$\theta_p^{\text{cm}} = 30^\circ$ (variant 2)

0.6	1	0.59	0.15	4510	642	941	0.79	0.18
0.8	1	0.56	0.15	5270	640	1138	1.73	0.58
1.0	1	0.53	0.15	6444	662	1473	3.02	0.79
1.2	2	0.50	0.15	7800	658	1861	7.59	0.85
1.4	4	0.47	0.15	10236	662	2632	19.9	1.03
1.6	5	0.45	0.15	11586	664	3026	27.4	1.55
1.8	5	0.40	0.15	15686	673	4228	29.6	3.14
2.0	4	0.35	0.15	21823	679	6029	37.5	11.78
total								19.90

Table V (continue).

E_γ	I_e	P_γ	Σ	$C_{ } + C_{\perp}$	C_a	C_e	$\frac{\text{accid}}{\text{trues}}$	T
GeV	μA			counts	counts	counts	%	hours

$$\theta_p^{\text{cm}} = 60^\circ$$

0.6	1	0.59	0.15	4908	739	1084	0.38	0.17
0.8	1	0.56	0.15	5448	759	1254	0.62	0.39
1.0	3	0.53	0.15	7079	771	1706	2.81	0.57
1.2	5	0.50	0.15	8742	777	2212	6.42	0.97
1.4	10	0.47	0.15	11522	796	3124	14.1	1.65
1.6	10	0.45	0.15	13293	809	3684	18.0	3.89
1.8	30	0.40	0.15	18227	816	5240	43.1	3.16
2.0	30	0.35	0.15	30633	1041	9545	40.7	12.03
							total	22.83

$$\theta_p^{\text{cm}} = 90^\circ$$

0.6	1	0.59	0.15	4882	728	1070	0.031	0.15
0.8	1	0.56	0.23	6190	1944	1455	0.041	0.55
1.0	5	0.53	0.20	7964	1654	2021	0.283	0.32
1.2	10	0.50	0.15	10206	979	2758	1.040	0.45
1.4	30	0.47	0.15	14548	1100	4304	3.522	0.49
1.6	30	0.45	0.15	18222	1229	5624	2.335	1.20
1.8	50	0.40	0.15	25438	1285	8101	3.694	1.73
2.0	50	0.35	0.15	35570	1335	11549	5.810	5.78
							total	10.65

Table V (continues).

E_γ GeV	I_e μA	P_γ	Σ	$C_1 + C_\perp$ counts	C_a counts	C_e counts	$\frac{\text{accid}}{\text{trues}}$ %	T hours
$\theta_p^{\text{cm}} = 120^\circ$								
0.6	1	0.59	0.15	6278	1117	1590	0.041	0.13
0.8	1	0.56	0.15	7722	1191	2047	0.050	0.40
1.0	2	0.53	0.15	9943	1304	2799	0.147	0.62
1.2	5	0.50	0.15	13899	1530	4226	0.598	0.77
1.4	20	0.47	0.15	22566	1960	7597	2.778	0.65
1.6	30	0.45	0.15	25246	1901	8545	4.952	0.98
1.8	30	0.40	0.15	40534	2286	14465	6.005	2.49
2.0	50	0.35	0.15	54092	2139	19536	15.53	4.93
total								10.97
$\theta_p^{\text{cm}} = 150^\circ$								
0.6	1	0.59	0.15	8094	1647	2291	0.077	0.12
0.8	1	0.56	0.15	10288	1832	3056	0.088	0.34
1.0	2	0.53	0.15	13934	2104	4396	0.244	0.51
1.2	5	0.50	0.15	19193	2367	6400	0.871	0.60
1.4	10	0.47	0.15	40120	3988	15141	2.372	1.09
1.6	20	0.45	0.15	36100	2962	13171	8.625	1.09
1.8	30	0.40	0.15	54379	3251	20459	18.14	1.74
2.0	30	0.35	0.15	82154	3549	31598	36.98	5.93
total								11.42

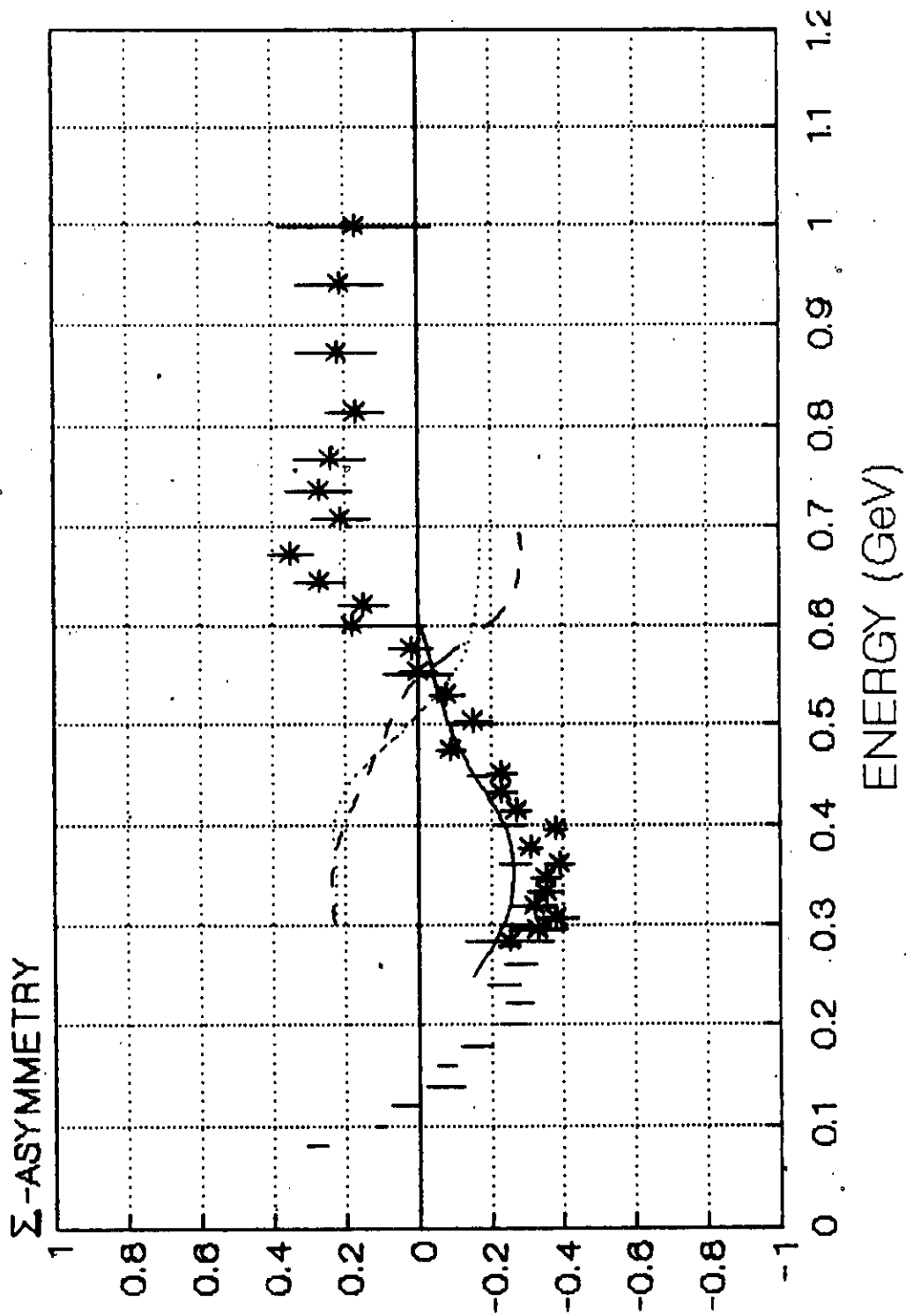


Fig. 1a. Asymmetry of the cross section of the reaction $d(\gamma, p)n$ at $\theta_p^{\text{cm}} = 90^\circ$. Experimental data:
 | - from ref. [4]; * - from ref. [12]. Theoretical curves: — - from ref. [10]; -
 from ref. [15]; --- - from ref. [8] with two dibaryon resonances $1(3^-)$ and $0(3^-)$.

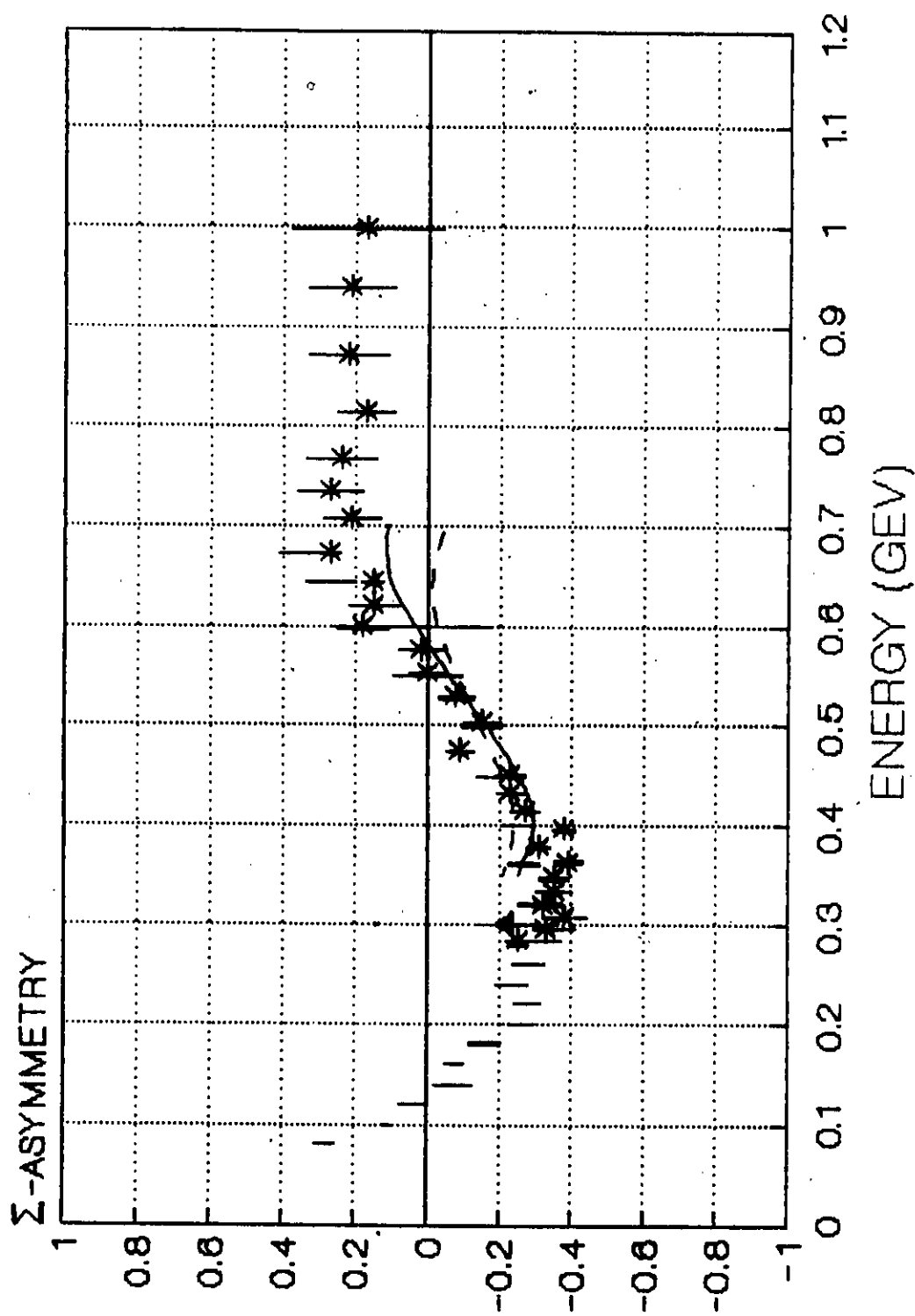


Fig.1b. The same as in fig.1a. Theoretical curves from ref. [9]: --- - without dibaryon resonances; — - with $1(2^+)$, $1(3^-)$ and $0(3^+)$ resonances. * - our data, obtained on mixed $\gamma^+ e^-$ beam Kharkov, 1991.

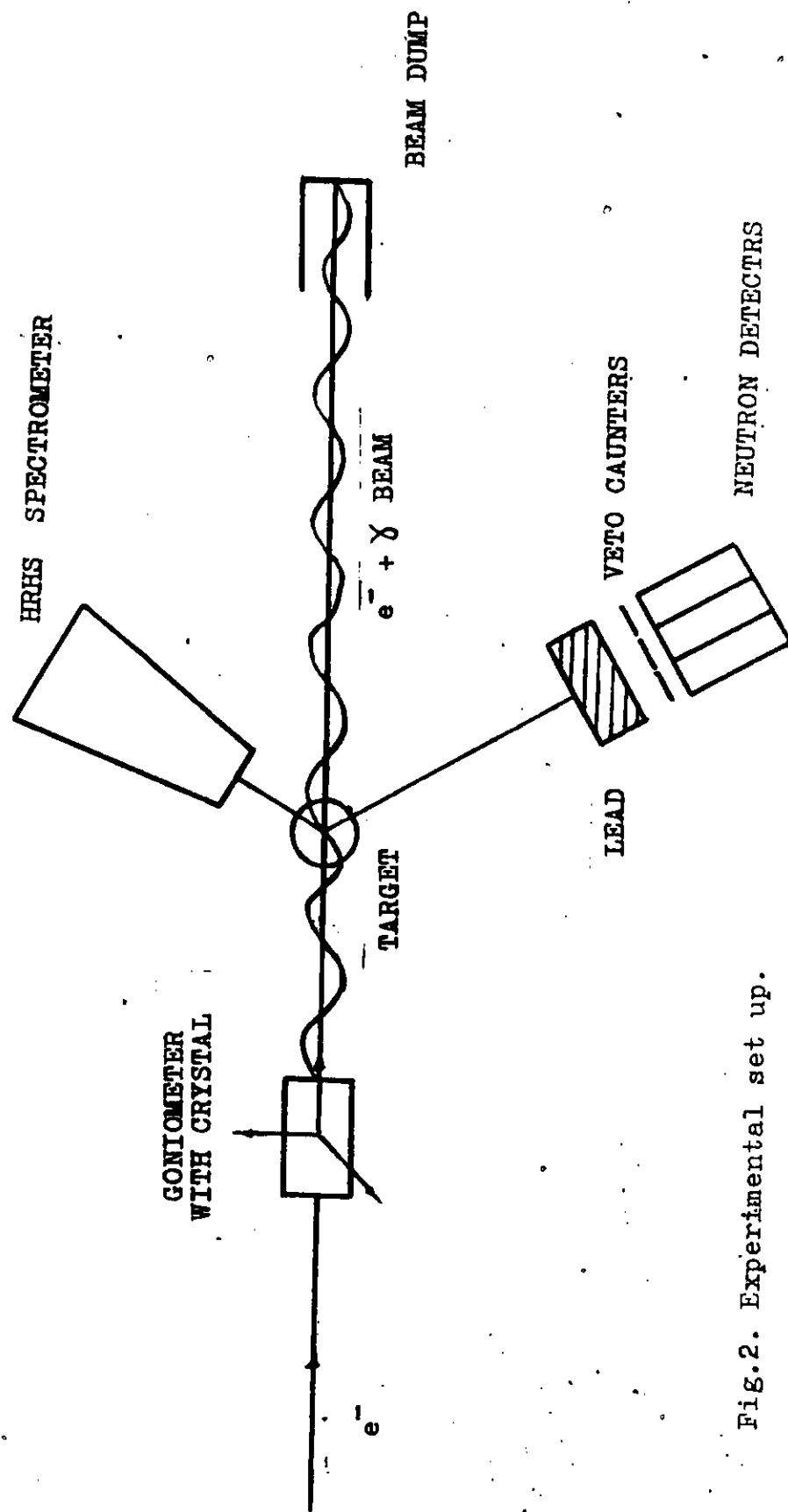


Fig.2. Experimental set up.

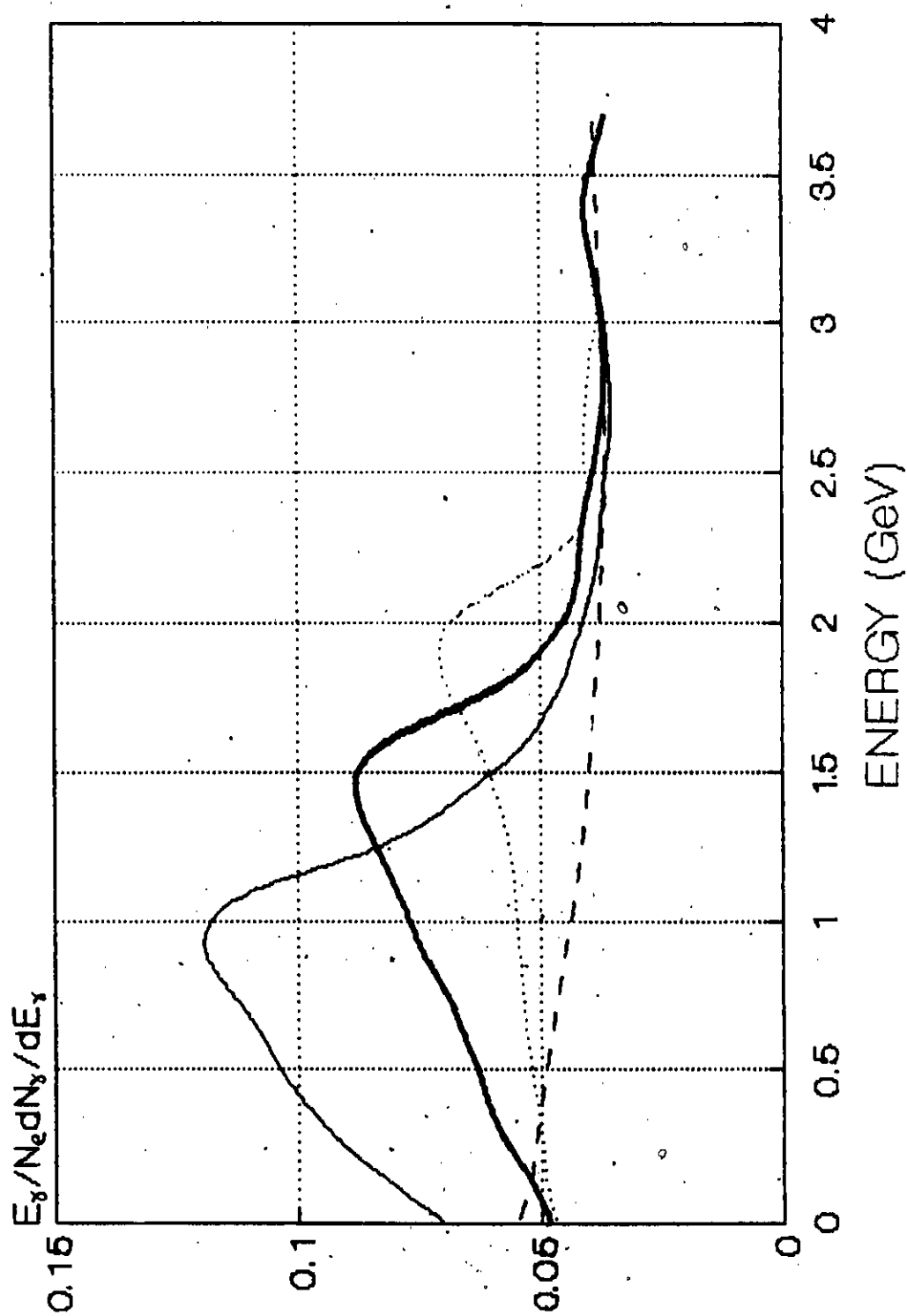


Fig.3a. Spectra of coherent bremsstrahlung for electron energy $E_0 = 4$ GeV and peak photon energies 1 GeV (—), 1.5 GeV (---), 2 GeV (.....). Diamond, orientation (2,2,0), thick 6 mm.---- bremsstrahlung spectrum.

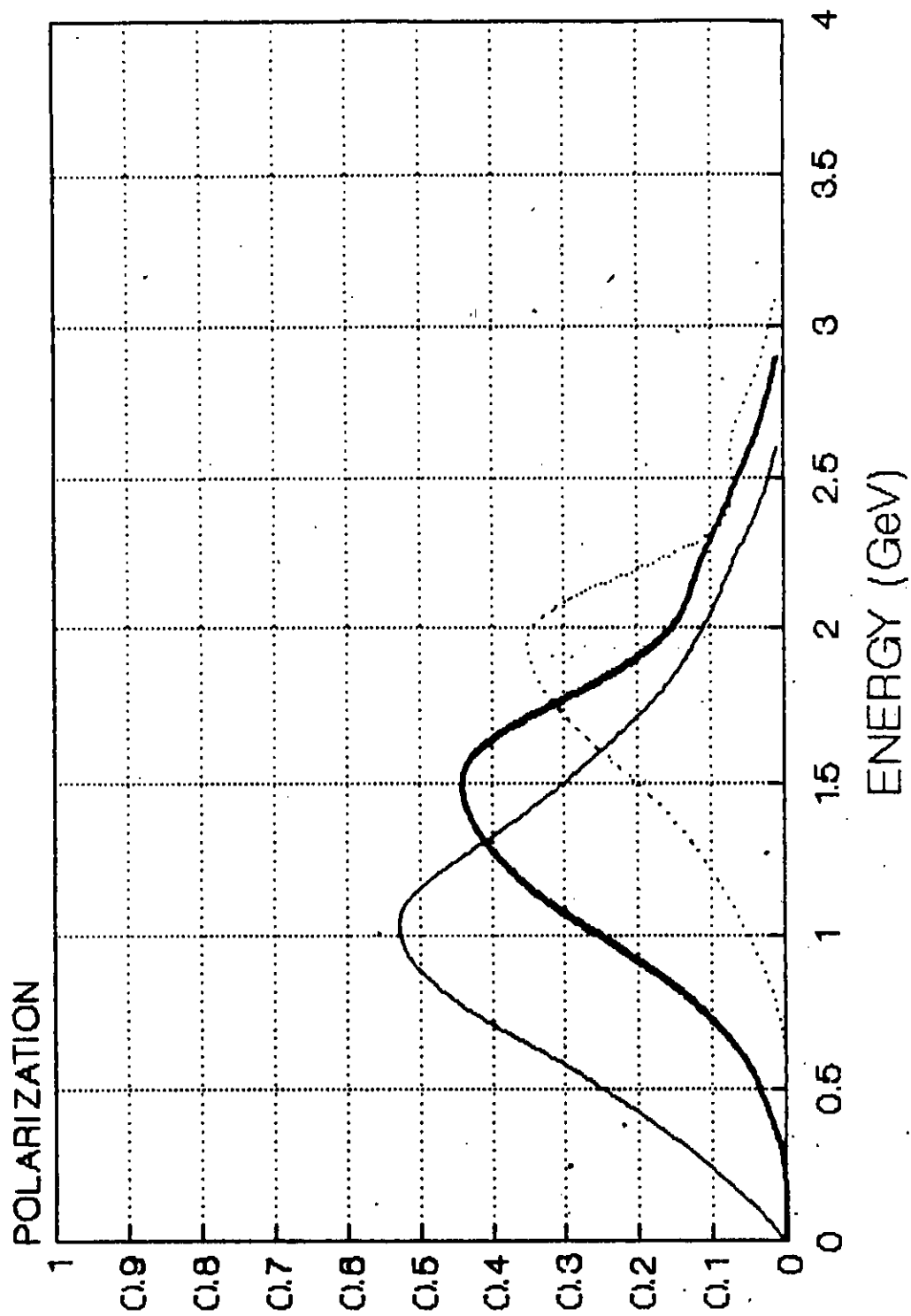


Fig.3b. Polarization of coherent bremsstrahlung. Notation and conditions the same as in fig.3a.

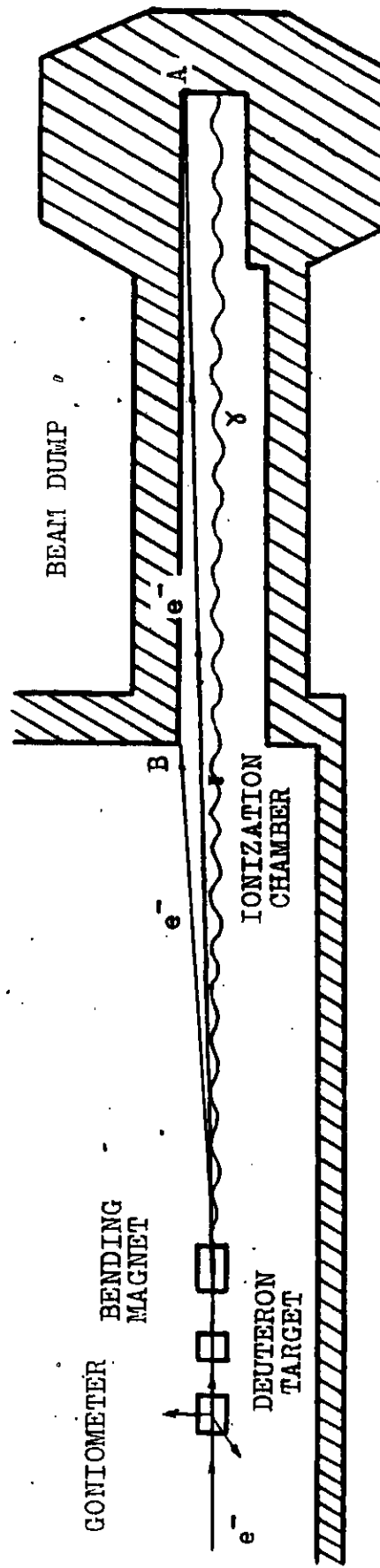


Fig.4. Experimental set up for crystal orientation.

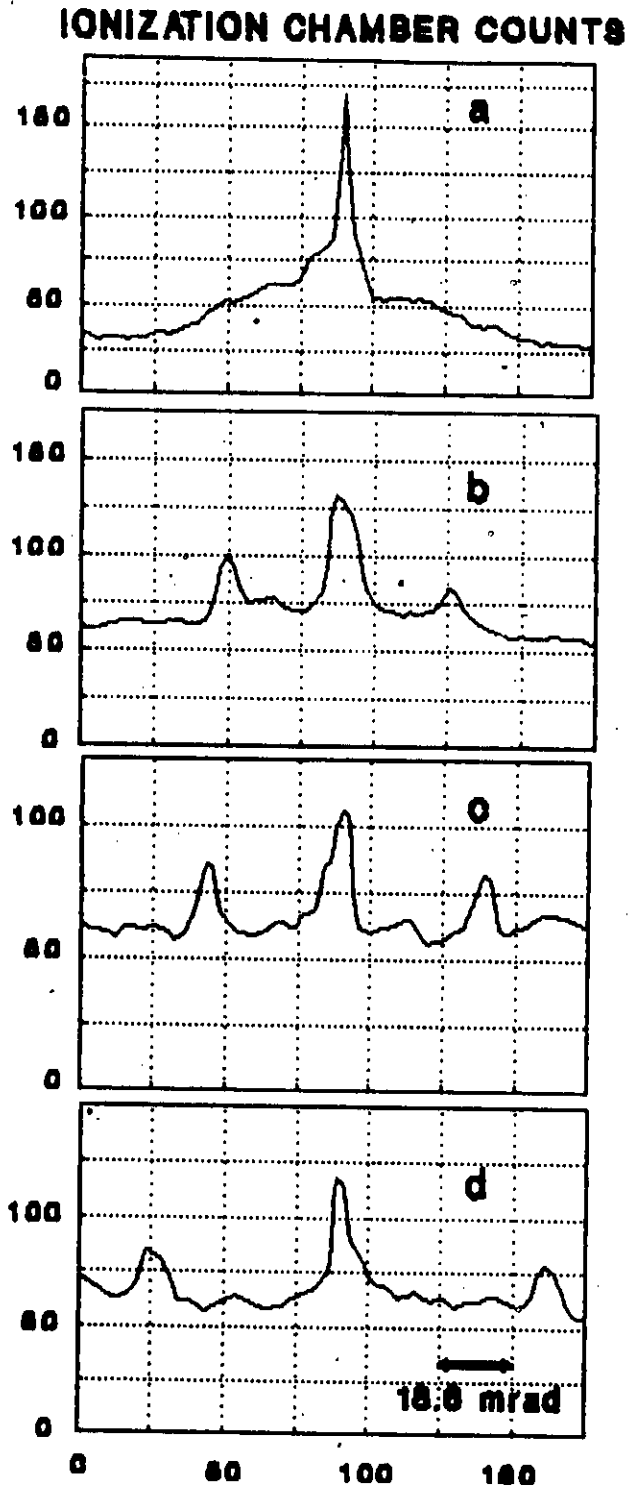


Fig.5. Orientation dependences of counts of ionization chamber when electron beam is deflected by bending magnet after passing through the crystal. $E_0 = 1.2$ GeV. a) $\phi = 0$ (axial orientation); b) $\phi = 15.6$ mrad; c) $\phi = 23.6$ mrad; d) $\phi = 27.6$ mrad.

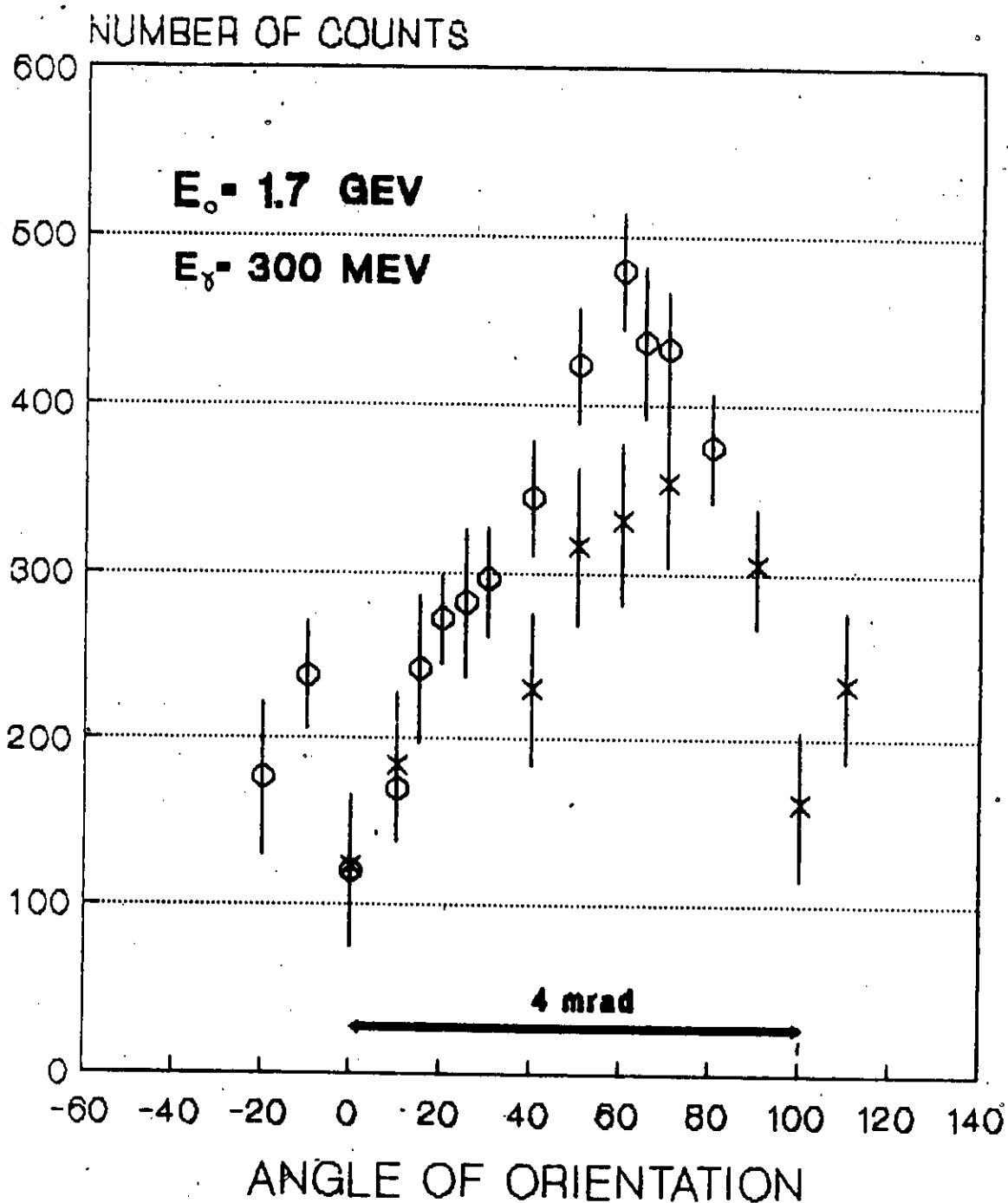


Fig.6. Orientation dependencies of proton yields from reaction photo-disintegration of the deuteron. ϕ (*) - polarization vector of the γ - beam perpendicular (parallel) to the reaction plane. $\theta_p^{cm} = 90^\circ$.